

DAA / LANGLEY

1NAG1-659

(NASA-CR-180348) MICROMECHANICS OF
COMPOSITE LAMINATE COMPRESSION FAILURE
Semiannual Progress Report, period ending 1
Nov. 1986 (Texas A&M Univ.) 37 p Avail:
NTIS HC A03/EF A01

N87-26977

Unclas

CSC1 11D G3/24 0063722

Semi-Annual Progress Report

for

NASA Research Grant NAG-1-659

entitled

**MICROMECHANICS OF COMPOSITE LAMINATE
COMPRESSION FAILURE**

prepared by

E. Gail Guynn
Walter L. Bradley
Department of Mechanical Engineering
Texas A&M University
College Station, TX 77843
(409) 845-1259

(for work through November 1, 1986)

November 15, 1986

Contract Monitor: John Whitcomb
Nasa Langley

1.0 OBJECTIVES

The objectives of this proposed research program are as follows:

- 1.1 to better define the micromechanics of compressive failure in composite materials;
- 1.2 to evaluate the accuracy with which the growth of shear-crippling or other types of damage that precedes final compressive failure can be predicted by current models; and
- 1.3 to develop where necessary new models to predict compressive failure in composite laminates.

2.0 SUMMARY OF ACCOMPLISHMENTS

04/01/86 THROUGH 11/01/86

The Dugdale analysis for metals loaded in tension has been adapted to model the failure of notched composite laminates loaded in compression. Compression testing details, MTS alignment verification, and equipment needs have been resolved. Thus far, only 2 (rather than 3) ductile material systems, HST7 and F155, have been selected for study. A Wild M8 Zoom Stereomicroscope and necessary attachments for video taping and 35mm pictures have been purchased. Currently, this compression test system is fully operational. A specimen is loaded in compression, and load vs. shear-crippling zone size is monitored and recorded. Data from initial compression tests indicate that the Dugdale model does not accurately predict the load vs. damage zone size relationship of notched composite specimens loaded in compression.

3.0 INITIAL MODEL BASED ON DUGDALE ANALYSIS

3.1 BACKGROUND

Compression fracture tests to determine the loading-rate effects on composite materials were completed at NASA Langley Research Center [Gynn and Elber, 1985]. Specimens tested were 1" wide with a 1.5" gage length, each containing a center hole. Hole diameters used in this study were 1/32", 1/16", 1/8", and 1/4". The specimens were loaded in compression to failure in a servo-controlled hydraulic test stand under load-control. From preliminary results, the loading rate was predetermined so that the ramp time to failure for each test was approximately 1, 10, 100, 1000, 10000, or 100000 seconds. These specimens were tested in a laterally stiffened grip system as shown in Figure 1. To provide lateral alignment, the two grips were connected using linear bearings and close tolerance matching rods. Elevated temperature tests were conducted with the grip system enclosed in an oven at 250°F. Two brittle (Narmco 5208 and 1808I matrices) and two ductile (General Electric Company ULTEM and Imperial Chemical Industries PEEK matrices) material systems were tested.

An example of typical data from this series of tests is shown in Figure 2. From this type of plot, temperature and loading rate effects were studied for each material and each hole size. A linear regression analysis was used to determine the best linear fit to the data. The 3 compressive failure modes observed were the multi-interleaf (brooming) in brittle systems and the shear-crippling or driving wedge in ductile systems, as shown in Figure 3.

3.2 OBSERVATIONS OF THE COMPRESSION FAILURES

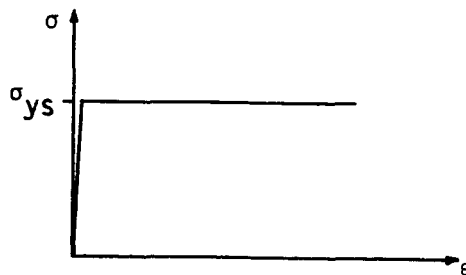
In these compression tests, a damage zone, similar to a flat fatigue crack in metals, initiates at the edges of the hole and propagates across the

width of the specimens to yield final failure. The length or size of this zone increases with increasing compressive load. The damage zone is virtually symmetric (ignoring load and specimen assymetry) about the hole and, it is initiated by local fiber buckling and/or shear crippling in the edges of the hole. Figure 4 shows the initiation and propagation of this damage zone across the specimen's width. However, this damage zone was observed only in the two ductile material systems (PEEK and ULTEM). It was observed [Guynn and Elber, 1985] that stable growth of the shear-crippling zone in brittle systems is very short and cannot be optically detected prior to catastrophic failure. The appearance of the ductile compression failures is very similar to the Dugdale plastic zone model. Thus, the Dugdale model was applied to ductile notched composite laminates loaded in compression.

3.3 DUGDALE MODEL

In this section the derivation of the Dugdale model will be reviewed [1, 2, 3]. An analytical solution for the Dugdale model will be obtained for a through crack in a wide plate. The assumptions of the model are as follows:

3.3.1 The material is elastic-perfectly plastic; i. e., no strain hardening.



3.3.2 The stress state is plane stress, requiring the plate to be relatively thin.

3.3.3 The geometry is a through crack in a wide plate.

3.3.4 The plastic zone is a long narrow strip ahead of crack tip.

This shape is defined as a Dugdale type zone, and is more likely to be found in polymeric materials because of the variation in yield strength with hydrostatic tension.

Dugdale assumed an effective crack length which is longer than the physical crack as shown in Figure 5. The assumption was that an actual center crack of length $2a$ could be modeled as a crack of length $2(a + \rho)$, where ρ is the length of the plastic zone ahead of the crack tip. Furthermore, this plastic zone could be modeled as a crack with compressive surface tractions equal to the yield stress, σ_{ys} , of the material. The size of ρ is selected so that the stress intensity associated with the compressive loading exactly cancels the stress singularity associated with the applied tensile stress yielding a finite stress distribution in the coupon. This condition of compatibility is expressed as follows:

$$K_{\sigma} = -K_{\rho} \quad \text{or} \quad K_{\sigma} + K_{\rho} = 0 \quad (1)$$

and is illustrated in Figure 6.

A crack with an internal tensile stress p distributed across its length has a stress intensity factor equal to

$$K_I = p\sqrt{\pi a} . \quad (2)$$

The Dugdale approach is modeled as a crack with internal wedge pressure. This pressure acts as a series of evenly distributed wedge forces, P (force per unit plate thickness), as illustrated in Figure 7. The general solution for an eccentric point force may be described by Green's function and is given by

$$K_{IA} = \frac{P}{\sqrt{\pi a}} \sqrt{\frac{a+x}{a-x}} \quad \text{and} \quad K_{IB} = \frac{P}{\sqrt{\pi a}} \sqrt{\frac{a-x}{a+x}} \quad (3)$$

where K_{IA} and K_{IB} are the stress intensity factors for crack tips A and B

respectively.

For a uniformly applied internal pressure, one may assume that the pressure p acts as a series of evenly distributed crack opening forces from s to the crack tip (as in the Dugdale case). Then, K may be determined from the following integration over the crack surface:

$$K = \int_s^a (K_{IA} + K_{IB}) dx = \int_s^a \frac{p}{\sqrt{\pi a}} \left[\sqrt{\frac{a+x}{a-x}} + \sqrt{\frac{a-x}{a+x}} \right] dx \quad (4)$$

$$K = 2P \frac{\sqrt{a}}{\sqrt{\pi}} \int_s^a \frac{dx}{\sqrt{a^2 - x^2}} \quad (5)$$

The integration is carried out by a change of variable, $x = a \cos \phi$, and the solution is

$$K = 2P \frac{\sqrt{a}}{\sqrt{\pi}} \cos^{-1}(x/a) \Big|_s^a = p\sqrt{\pi a} \quad (6)$$

which is the same as (2).

Applying (6) to the Dugdale crack of Figure 5, the integral must be taken from $s = a$ to $(a+\rho)$. Thus, a must be substituted for s , $(a+\rho)$ for a and $-\sigma_{ys}$ for P . Therefore,

$$K_\rho = -2\sigma_{ys} \sqrt{\frac{a+\rho}{\pi}} \cos^{-1} [a/(a+\rho)] \quad (7)$$

From Figure 6c,

$$K_\sigma = \sigma \sqrt{\pi(a+\rho)} \quad (8)$$

According to (1), $K_\sigma = -K_\rho$ and thus,

$$\sigma \sqrt{\pi(a+\rho)} = 2\sigma_{ys} \sqrt{\frac{a+\rho}{\pi}} \cos^{-1} [a/(a+\rho)] \quad (9)$$

which reduces to

$$\frac{a}{a+\rho} = \cos \left[\frac{\pi \sigma}{2 \sigma_{ys}} \right] \quad (10)$$

Neglecting higher order terms of the infinite series for cosine, one may further reduce (10) to

$$\rho = \frac{\pi^2 \sigma^2 a}{8 \sigma_{ys}^2} = \frac{\pi K^2}{8 \sigma_{ys}^2}. \quad (11)$$

3.4 APPLICATION OF THE DUGDALE MODEL

The Dugdale model has been applied to ductile notched composite laminates loaded in compression because their failures resemble a flat fatigue crack in metals except that the stress directions are reversed. An example of this damage zone was shown in Figure 4. The fiber buckling zone (hereafter, crush zone) at each edge of the hole is compared to the plastic zone in metals. We have assumed that although the fibers are broken, the debris in the crush zone continues to carry load. Thus, one might assume that as the crush zone grew across the specimen width, a constant crushing pressure σ_0 would exist over the length of ρ .

Newman [3] applied the Dugdale approach to (1) a crack in a finite plate and (2) to cracks emanating from a circular hole in a finite plate. His result for cracks emanating from a circular hole in a finite width specimen is

$$S_{\max} F_h^S F_w^S - \alpha \sigma_0 \left[1 - \frac{2}{\pi} \sin^{-1}(c/d) \right] F_h^\sigma F_w^\sigma = 0 \quad (12)$$

where the geometry for this solution is shown in Figure 8.

For a given S_{\max} , w , r , c , α , and σ_0 , equation (12) is solved for d using an

iterative technique. However, $\rho = d - c$, and thus, the plastic zone size ρ is determined.

Initially, the work of this grant has followed Newman's analysis for cracks emanating from a circular hole in a finite width specimen, but the notched composite laminates were modeled with $c = r$. However, instead of using an iterative solution, curves of S_{\max} versus ρ were generated with σ_0 as a parameter for the various hole sizes. The rearranged solution for equation (12) follows:

$$S_{\max} = \frac{\alpha \sigma_0 \left[1 - \frac{2}{\pi} \sin^{-1}(c/d) \right] F_h^\sigma F_w^\sigma}{F_h^s F_w^s} \quad (13)$$

$$\text{where } \rho = d - c. \quad (14)$$

Appendix A details the nomenclature, specimen configuration (Figure A.1), and geometry requirements for this solution. Appendix B contains the listing of the computer program which generates the theoretical curves of S_{\max} vs. ρ . Figure B.1 shows an example of the curves generated for each particular hole size.

4.0 RESULTS FROM NASA WORK AT TAMU

Data from two compression tests at Texas A&M University are presented in Figures 9 and 10. NASA Langley (John Whitcomb) presently has a VHS video tape of the specimen failed in Figure 10. From these plots, it is obvious that the Dugdale model does not accurately predict the load-damage zone size relationship of notched composite specimens loaded in compression.

Possible reasons that this model does not exactly fit the data are as follows:

4.1 The constitutive relationship used in the Dugdale model is not an

accurate description of material response in the crush zone.

- 4.2 The crush zone was only measured on one side of the specimen. Since the actual crush zone is not perfectly symmetric, ρ should be the average of 4 measurements, 2 on each side of the specimen.

5.0 WORK PLANNED FOR REMAINDER OF THIS CONTRACT YEAR

Future work on this grant includes:

- 5.1. testing 3 ductile material systems containing 3 hole sizes per material;
- 5.2 determining a three-dimensional schematic of the damage zone using sectioning techniques and electron microscopy;
- 5.3 developing a better model for these compression failures;
- 5.4 verifying the agreement between the model and the test data for the 3 ductile material systems.

5.5 EXPERIMENTAL FACILITIES

This section details the fully operational equipment and materials presently available for the completion of the work of this grant.

5.5.1 Equipment

The damage development adjacent to the center hole which precedes final failure is monitored using a newly acquired Wild M8 Zoom Stereomicroscope. This system includes magnification of 2.4X to 160X at working distances of 1" to 7", respectively, with capability for 35mm pictures and Beta or VHS format video recording of the damage development. The specimens are illuminated with one of two sources, either a fiber optics system oblique to the specimen or a coaxial system perpendicular to the specimen to detail surface relief. This system is shown in Figure 11. In order to monitor both sides of the specimen

simultaneously, a rotating mirror is being added to this system. To quantify the strain fields around the damage, or crush zone, an interferometric system will be added to our present experimental set up. This information should allow us to determine through the thickness damage before it is visible on the surface of the specimen. Dr. Chris Burger will assist in the implementation of this capability which will allow the measurement of (1) out-of-plane displacements and (2) in-plane strains. Furthermore, an acoustic emission device will be added to the specimen to aid in the detection of microbuckling, prior to any visible surface damage.

5.5.2 Materials

The present 48-ply panel of AS4/PEEK, $[\pm 45/0_2/\pm 45/0_2/\pm 45/0/90]_{2S}$, has been sacrificed for trial-and-error specimens to get the system operating optimally. Additionally, the panel has not exhibited the ductile characteristics observed in previously tested panels of ICI PEEK. The future work of this grant will compare data from 3 ductile material systems, 3 hole sizes per material. However, the best comparison will be accomplished if the 3 material systems have the same stacking sequence. Furthermore, the interferometric techniques may be optimized by applying a fine mesh of scrim cloth to the panel surfaces when the panels are manufactured. The stacking sequence selected is $[(0/\pm 45/90)_S]_4$. Presently, one panel of T6C145/F155 (prepreg supplied by Hexcel) has been manufactured at Texas A&M University, and we are expecting one panel of HST7 interleaf material from Bell Helicopter in Fort Worth, Texas. Additionally, NASA Langley has agreed to supply the third panel of a ductile material system of the same stacking sequence.

5.6 BULK DAMAGE ZONE ASSESSMENT

5.6.1 Introduction

Compression failures in notched composite laminates are preceded by the development of a damage zone which grows with increasing compressive load. This damage zone is adjacent to the center hole and is initiated by local fiber buckling and/or shear crippling in the edges of the hole. As the compressive load increases, the damage zone progresses across the width of the specimen to final failure. Although the final compressive failure modes have been observed and reported [4], the details of the damage progression and development prior to catastrophic failure remain unclear. Micrographs of GR/PEEK [5] and buckled 0^0 fibers in composite laminates [4] exist, but details of the scanning electron microscope (SEM) conditions are not included. The purpose of this study is to section through the thickness of a damaged specimen, examine each section in the SEM, and determine the extent of the fiber buckling zone.

5.6.2 Materials and Methods

The laminate selected for this study consists of high strain carbon fibers (AS4) embedded in a semi-crystalline thermoplastic known as polyetheretherketone (PEEK). PEEK is an aromatic polyether resin which is primarily useful because of its exceptional toughness as well as chemical resistance. PEEK is sold under the trade name "Victrex" PEEK by Imperial Chemical Industries, Limited (ICI) - United Kingdom and recently became available in 1981 [6]. The particular specimen selected for this study is a 48-ply notched composite laminate of AS4/PEEK. The laminate stacking sequence is $[\pm 45/0_2/\pm 45/0_2/\pm 45/0/90]_{2S}$. This material was supplied by the grant sponsor, NASA Langley Research Center - Hampton, Virginia, but originally manufactured by ICI.

Compression tests have been conducted in a specially designed ultra high axial alignment MTS (Material Test System) machine in the Materials and Structures Laboratory of Texas A&M University. The specimens tested were loaded in compression to failure in the servo-controlled hydraulic test stand under displacement control at a relatively slow rate of 0.001 in./min. to provide more stable growth of the shear-crippling zone. The damage development adjacent to the center hole which preceded final failure was monitored using the Wild M8 Zoom Stereomicroscope. Prior to catastrophic failure, some tests were interrupted to provide specimens with significant damage for sectioning studies of the shear-crippling zone.

Compression specimens tested were 1" wide with a 2" gage length, each containing a center hole. Hole diameters were 1/16", 1/8", and 1/4". A specimen containing a fiber microbuckling zone of significant size has been selected to section. This specimen is 0.24" thick and has a center hole of diameter 0.125". Figure 12a shows a detailed schematic of the specimen configuration. In order to section through the damage zone, the center one-quarter-inch of length (Figure 12b) will be cut from the compression specimen using a Struers Accutum Precision Saw (diamond blade). This horizontal center section will be cut along its vertical centerline into two halves. Each of these halves will be mounted in a plastic stub. One half will be sectioned and studied through the thickness of the laminate while the other half will be sectioned across the width of the specimen from the edge of the hole to the edge of the specimen. The two sections will then be studied in a Jeol 25 Scanning Electron Microscope. The Struers Precision Saw will be utilized for the major sectioning cuts, while the thinner cuts and final polishing (preparation for SEM) will be accomplished using a microprocessor controlled grinding and polishing machine also manufactured by Struers (Abramin Automated

Polishing Unit).

The first observations in the SEM will be of the actual microbuckled zone, prior to any polishing. Initially, the two mounted specimens will be examined without a conductive coating to determine if an acceptable SEM image (particularly no charging) is possible. Because of the high conductivity of the carbon fibers and low conductivity in the resin and plastic mount, it is expected that each specimen surface will need to be sputter coated with a layer of gold palladium approximately 200Å thick. Since the fibers are buckled out of plane of the specimen, a long working distance (48mm) and small aperture will be selected to obtain maximum depth of field for these first micrographs. The highly polished surfaces resulting from the sectioning process may make it possible to observe the specimen sections using the shorter working distance (10mm), thus allowing more resolution of each section. In all cases, the optimum accelerating voltage will be determined to obtain the best specimen image and still minimize specimen charging. Although experimental work on textile materials, metals, and thin films [7] shows the effects of varying the operating conditions of the SEM, optimum determination of the correct combination of these conditions for AS4/PEEK is expected to be a trial-and-error process.

5.7 ADAPTING MODEL

Future work on this grant will include an attempt to develop a model which will better describe the relationship between the remotely applied compressive stress and the growth in the crush zone size. Possible solutions are as follows:

1. Using interferometric techniques, determine strain distribution around, and if possible, in the crush zone. Paul Tan of Analytical

Services & Materials, Inc. (ASM) at NASA Langley is using his boundary element code to numerically determine the stress distribution around the holes. Our experimental results will be compared with his analytical results.

2. Different constitutive relationships for the crush zone may be postulated and incorporated in a finite element model to determine which one yields an accurate prediction of the size and shape of the damage zone as well as the surrounding strain field.
3. More quantitative criteria for the initiation of shear crippling as well as unstable propagation of this zone should also be forthcoming.

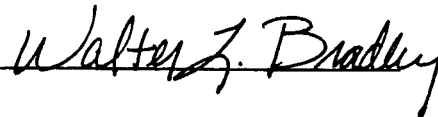
6.0 SUMMARY

Notched composite laminates of AS4/PEEK have been loaded in compression to failure. From the load-damage zone size data, it has been determined that the Dugdale analysis does not accurately predict this relationship. Future work includes the incorporation of a more realistic constitutive model which reflects these compression failures into a Dugdale type analysis, checking its accuracy for 3 material systems, each containing 3 hole sizes.

E. Gail Guynn



Walter L. Bradley



7.0 REFERENCES

- [1] D. Broek, Elementary Engineering Fracture Mechanics, Martinus Nijhoff Publishers, Boston, MA (1982).
- [2] W. L. Bradley, "Micromechanics of Fatigue and Fracture of Alloys," course at Texas A&M University, College Station, TX, (1986).
- [3] J. C. Newman, Jr., A Nonlinear Fracture Mechanics Approach to the Growth of Small Cracks. Behavior of Short Cracks on Airframe Components, AGARD Conference Proceedings, Paper CP328, pp. 6-1 to 6-26.
- [4] J. H. Starnes and J. G. Williams, "Failure Characteristics of Graphite-Epoxy Structural Components Loaded in Compression," Proceedings of 1st IUTAM Symposium on Mechanics of Composite Materials (1982), pp. 283-306.
- [5] B. Malik, A. Palazotto, and J. Whitney, "Notch Strength of GR/PEEK Composite Material at Elevated Temperatures," Proceedings 26th Structures, Structural Dynamics, and Materials Conference (1985), pp.203-210.
- [6] J. T. Hartness, "Polyetheretherketone Matrix Composites," SAMPE Quarterly (1983), January:33-36.
- [7] J. W. S. Hearle, B. Lomas, and J. T. Sparrow, "The Selection of Conditions for Examination of Specimens in a Scanning Electron Microscope," Journal of Microscopy (1970), 92:205-216.
- [8] R. Burghardt, "Scanning Electron Microscopy," course at Texas A&M University, College Station, TX, (1986).

APPENDIX A

DUGDALE MODEL NOMENCLATURE

and

SPECIMEN CONFIGURATION

NOMENCLATURE

- α = Constraint factor
- b_k = Dimensions for partially loaded crack, in. ($k = 1,2$)
- c = Half crack length, in.
- d = Half crack length plus compressive plastic zone width, in.
- F_h^S = Boundary-correction factor for the circular hole, due to remote uniform stress
- F_h^σ = Boundary-correction factor for a circular hole in an infinite plate, partially loaded crack
- F_w^S = Boundary-correction factor for a two symmetric cracks emanating from a circular hole in a finite-width plate subjected to a uniform stress
- F_w^σ = Boundary-correction factor for two symmetric cracks emanating from a circular hole in a finite width plate subjected to partial loading
- K = Stress intensity factor, psi- $\sqrt{\text{in}}$
- ρ = Length of compressive crush or damage zone, in.
- r = Hole radius, in.
- S_{max} = Remotely applied stress, psi
- σ_0 = Flow stress, psi
- w = Specimen half width, in.

GEOMETRY REQUIREMENTS

$$\lambda = \frac{r}{d} \quad \text{and} \quad \gamma = \frac{b}{d}$$

$$d = \rho + c$$

$$\frac{r}{w} \leq 0.5$$

$$\frac{d}{w} \leq 0.7$$

$$0 \leq \lambda \leq 1$$

$$\lambda \leq \gamma \leq 1$$

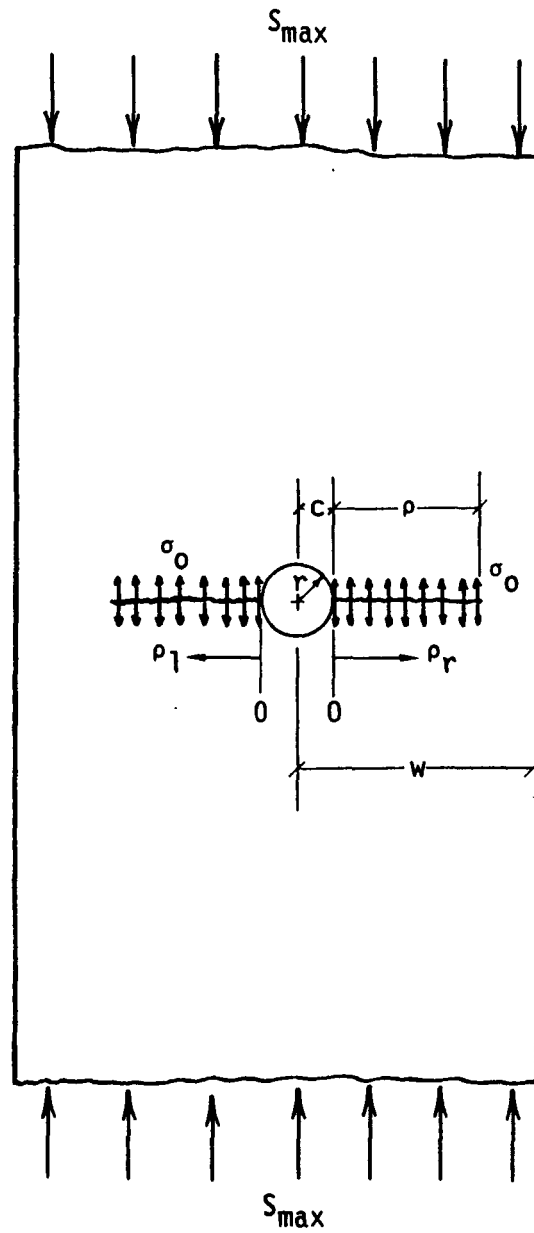


Fig. A. 1. Specimen configuration for the Dugdale model applied to open hole composite laminates loaded in compression.

APPENDIX B

PROGRAM LISTING

```

10 ! DUGDALE MODEL applied to composites in compression loading.
20 !
30 OPTION BASE 1
31 ! PLOTTER IS 13,"GRAPHICS"
32 PLOTTER IS 7,5,"9872A"
33 PENUP
34 SCALE 0,.50,0,100000
36 AXES .01,10000,0,0
40 ! PRINTER IS 0
50 IMAGE 3X,"SMAX,",2X,"ALPHA",2X,"HOLE RADIUS,",2X,"HALF WIDTH,",2X,"CRACK L
ENGTN,",3X,"RHO,",5X,"SIG0,"
60 !
70 IMAGE 4X,"PSI",15X,"IN",11X,"IN",12X,"IN",10X,"IN",6X,"PSI"
80 !
90 IMAGE 6D,6X,D,6X,D.DDDD,9X,D.DD,9X,D.DDDD,5X,D.DDDD,4X,6D
100 !
110 ! PRINT USING 50
120 ! PRINT USING 70
130 INPUT "Sig0, Alpha, R, W, C, Symmetric (Y or N)",Sig0,Alpha,R,W,C,N$
140 FOR Sig0=10000 TO 100000 STEP 10000
145 PENUP
150 FOR Rho=.001 TO .50 STEP .001
160 GRAPHICS
170 RAD
180 !
190 D=Rho+C
200 !
210 B1=C
220 B2=D
230 Lambda=R/D
240 !
250 F1=.707+.765*Lambda+.282*Lambda^2+.74*Lambda^3+.872*Lambda^4
260 !
270 F2=1+.358*Lambda+1.425*Lambda^2-1.578*Lambda^3+2.156*Lambda^4
280 !
290 IF N$="Y" THEN GOTO 350
300 !
310 Fn=F1
320 !
330 GOTO 50
340 !
350 Fn=F2
360 !
370 Fhs=Fn*SQR(1-Lambda)
380 !
390 Fws=SQR(1/COS(PI*R/2/W)/COS(PI*D/2/W))
400 !
410 A1=-.02*Lambda^2+.558*Lambda^4
420 !
430 A2=.221*Lambda^2+.046*Lambda^4
440 !
450 Gamma1=B1/D
460 !

```

```

470 Gamma2=B2/D
480 !
490 Con1=1+A1/(1-Lambda)+3*A2/2/(1-Lambda)^2
500 !
510 Con2=A1/(1-Lambda)+(4-Gamma2)*A2/2/(1-Lambda)^2
520 !
530 Con22=A1/(1-Lambda)+(4-Gamma1)*A2/2/(1-Lambda)^2
540 !
550 G=Con1*(ASN(Gamma2)-ASN(Gamma1))+Con2*SQR(1-Gamma2^2)-Con22*SQR(1-Gamma1^2
)
560 !
570 Fhsig=G/(ASN(Gamma2)-ASN(Gamma1))
580 !
590 Con3=PI*D/2/W
600 !
610 Bk1=SIN(PI*B1/2/W)/SIN(Con3)
620 !
630 Bk2=SIN(PI*B2/2/W)/SIN(Con3)
640 !
650 Con4=SQR(1/COS(Con3))
660 !
670 Fwsig=(ASN(Bk2)-ASN(Bk1))/(ASN(Gamma2)-ASN(Gamma1))*Con4
680 !
690 Smax=Sig0*Alpha*Fhsig*Fwsig*(1-2/PI*ASN(C/D))/Fhs/Fws
700 !
710 ! PRINT LIN(1)
720 !
721 PLOT Rho,Smax
730 ! PRINT USING 90;Smax,Alpha,R,W,C,Rho,Sig0
740 NEXT Rho
741 NEXT Sig0
750 GOTO 130
760 END

```

ORIGINAL PAGE IS
OF POOR QUALITY

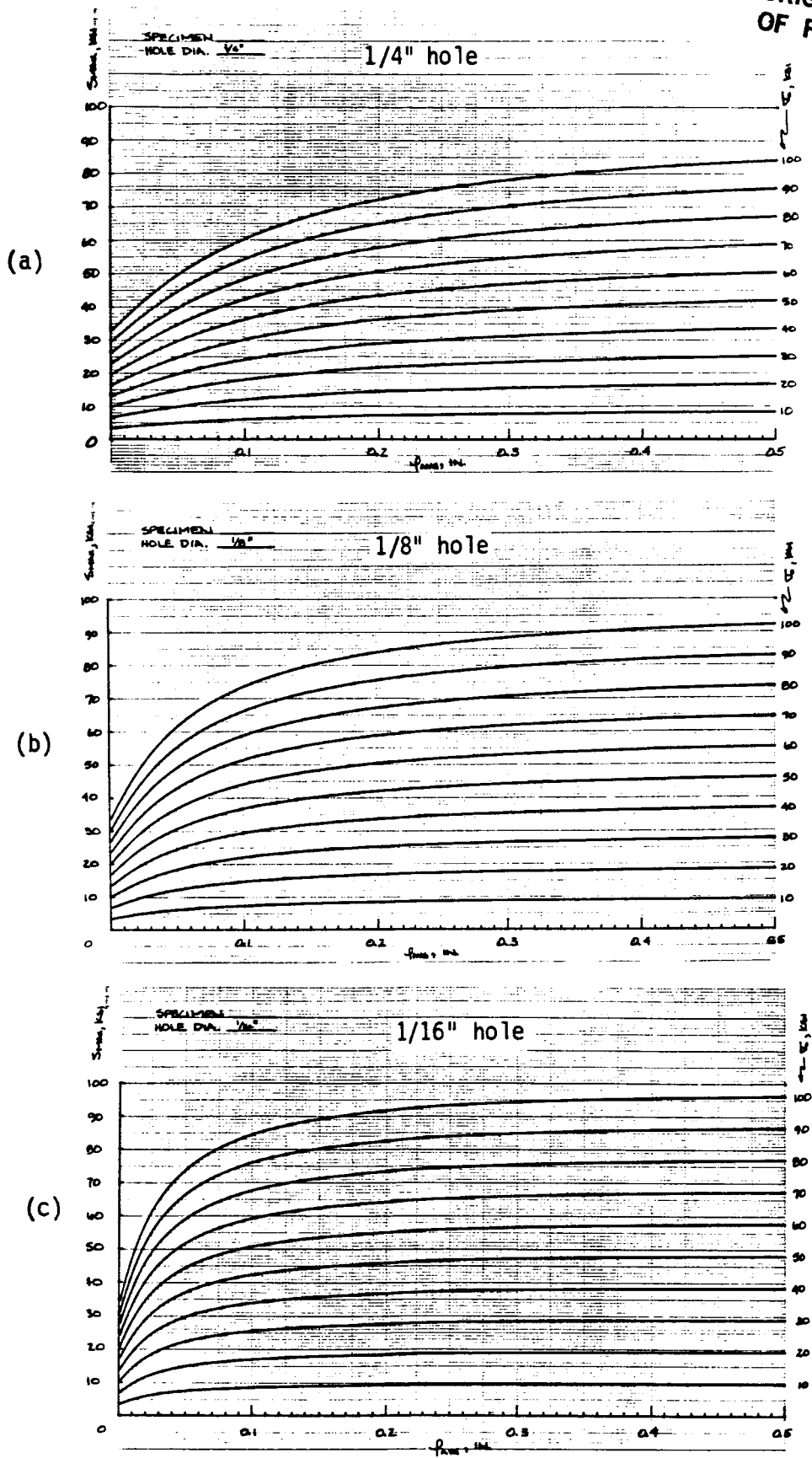


Fig. B. 1. Theoretical Dugdale curves of remote compressive stress vs. damage zone size with the crushing pressure as a parameter. (a) Hole diameter is 1/4". (b) Hole diameter is 1/8". (c) Hole diameter is 1/16".

LIST OF FIGURES

Fig. 1. Laterally stiffened linear-bearing grip system.

Fig. 2. Typical notched compressive strength-time to failure diagram illustrating temperature effects.

Fig. 3. Three types of final compressive failure modes. (a) Brooming in T300/5208. (b) Shear-crippling in AS4/PEEK. (c) Driving wedge in C12000/ULTEM.

Fig. 4. Initiation and propagation of damage zone prior to compressive failure in an AS4/PEEK specimen. Hole diameter is 0.0625". Damage zone lengths are (a) 0.020", (b) 0.030", (c) 0.050" and 0.120", and (d) 0.140" and 0.140".

Fig. 5. Dugdale crack.

Fig. 6. Crack tip stress intensity. (a) Stress singularity at crack tip of tensile loaded coupon. (b) Compressive stress intensity at crack tip attributed to compressive surface stresses over the plastic zone. (c) Finite stress distribution in tensile loaded coupon.

Fig. 7. Crack with applied wedge forces where P = force per unit plate thickness.

Fig. 8. Geometry for Newman's analysis.

Fig. 9. Applied compressive stress vs. crush zone size for 0.125" hole.

Fig. 10. Applied compressive stress vs. crush zone size for 0.125" hole.

Fig. 11. Compression test facility with stereomicroscope and video attachments.

Fig. 12. Specimen configuration. (a) Compression test specimen. (b) Specimen for sectioning studies.

Fig. A. 1. Specimen configuration for the Dugdale model applied to open hole composite laminates loaded in compression.

Fig. B. 1. Theoretical Dugdale curves of remote compressive stress vs. damage zone size with the crushing pressure as a parameter. (a) Hole diameter is 1/4". (b) Hole diameter is 1/8". (c) Hole diameter is 1/16".

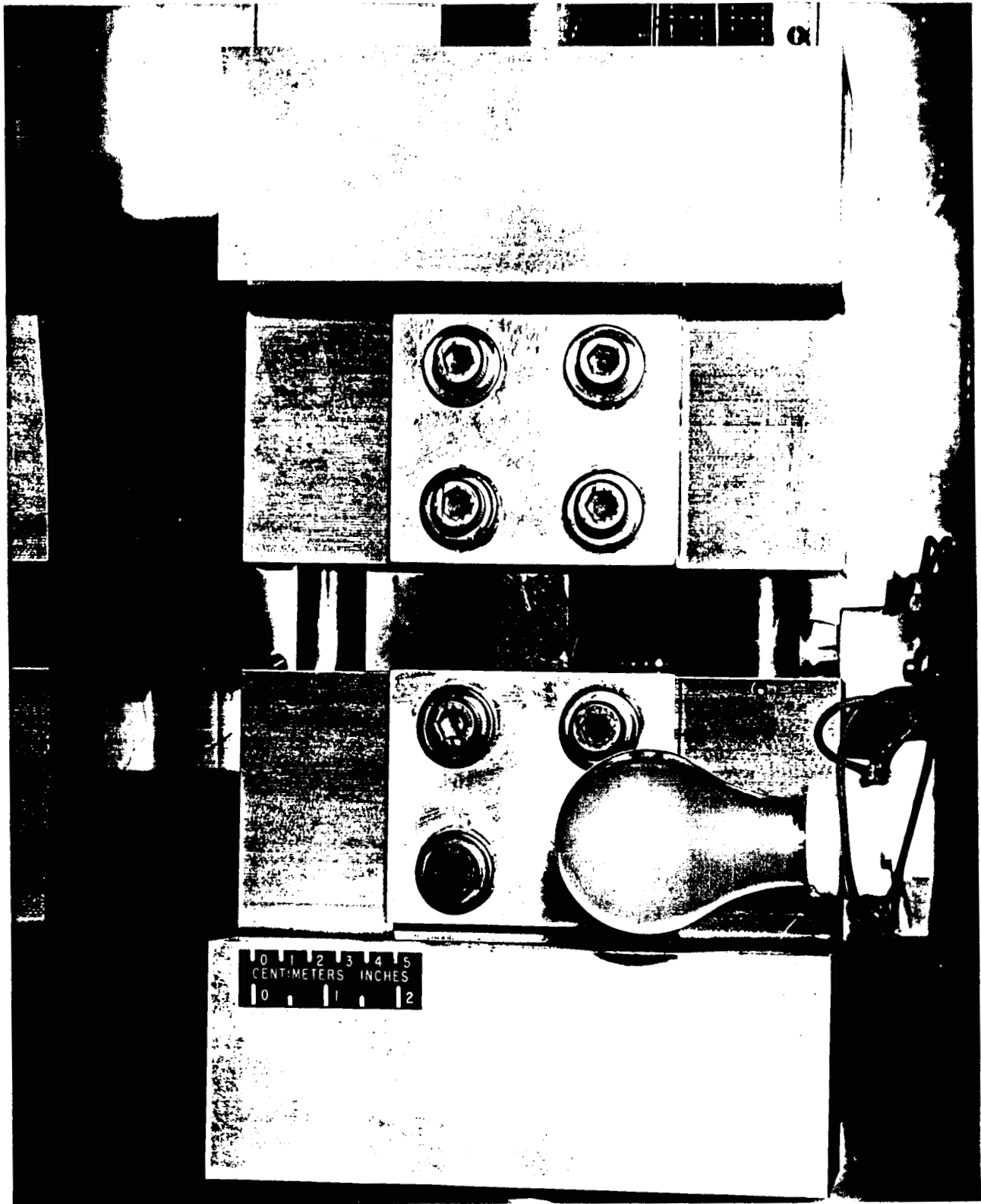


Fig. 1. Laterally stiffened linear-bearing grip system.

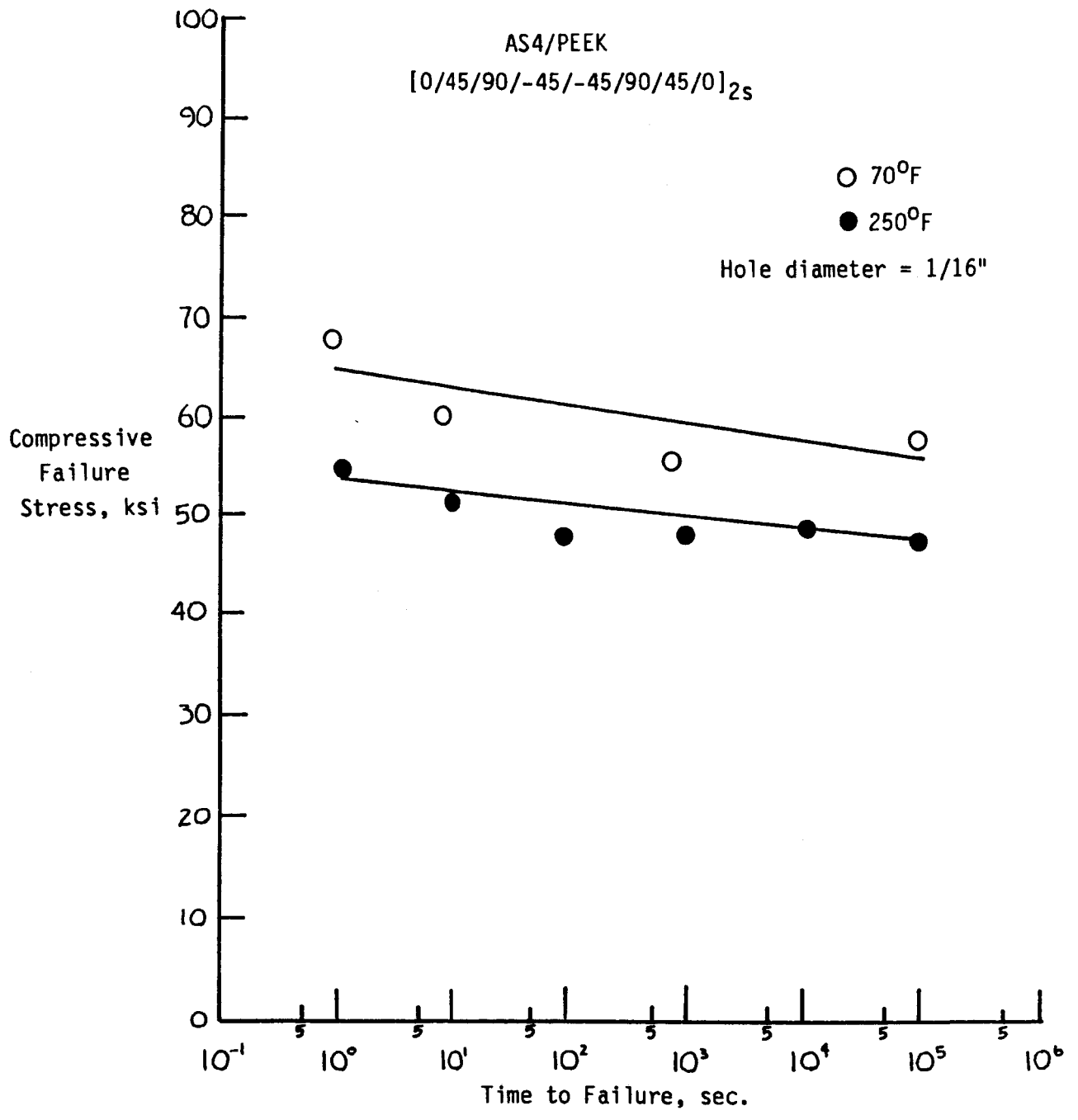


Fig. 2. Typical notched compressive strength-time to failure diagram illustrating temperature effects.

ORIGINAL PAGE IS
OF POOR QUALITY

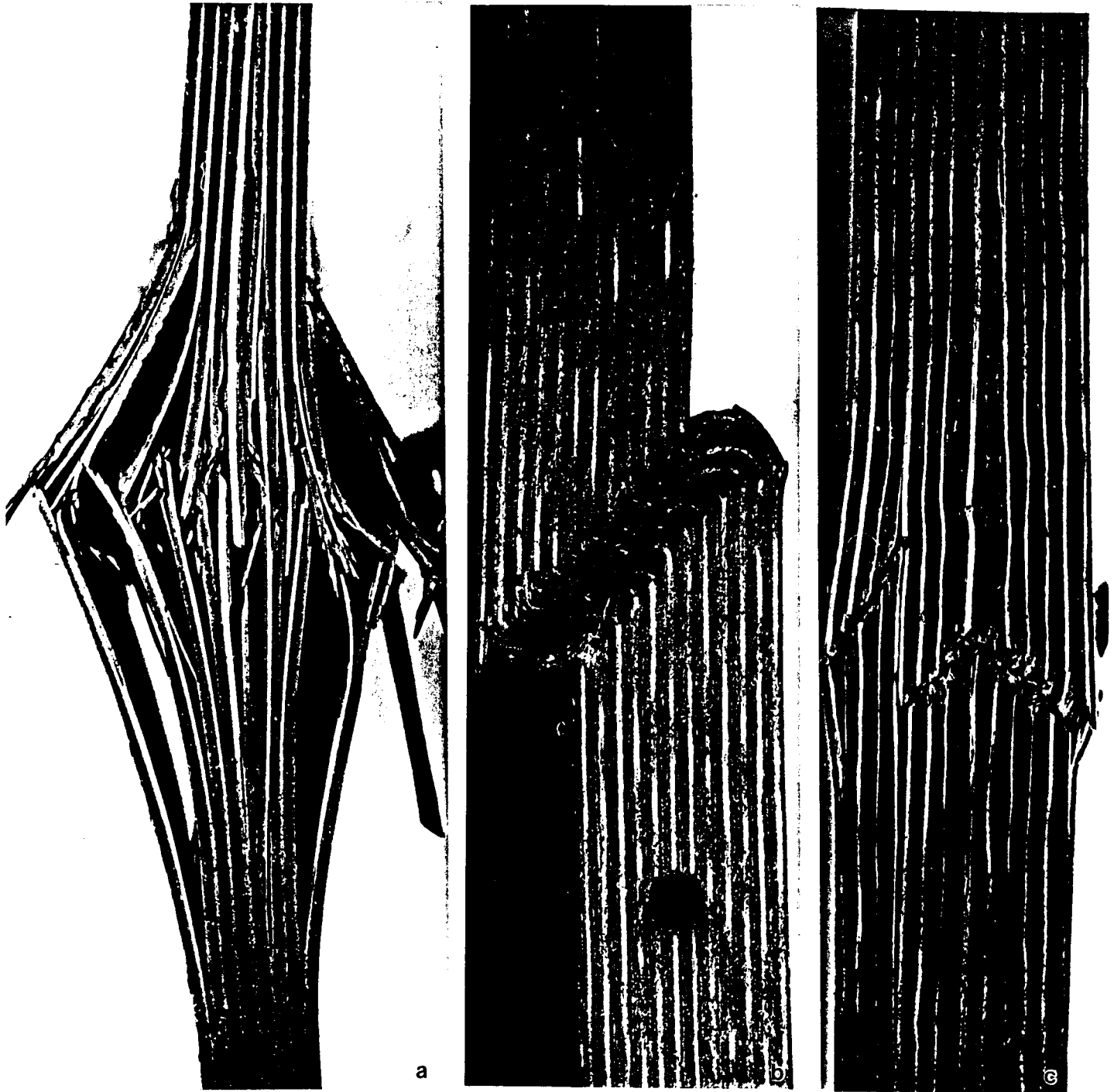


Fig. 3. Three types of final compressive failure modes. (a) Brooming in T300/5208. (b) Shear-crippling in AS4/PEEK. (c) Driving wedge in C12000/ULTEM.

ORIGINAL PAGE IS
OF POOR QUALITY

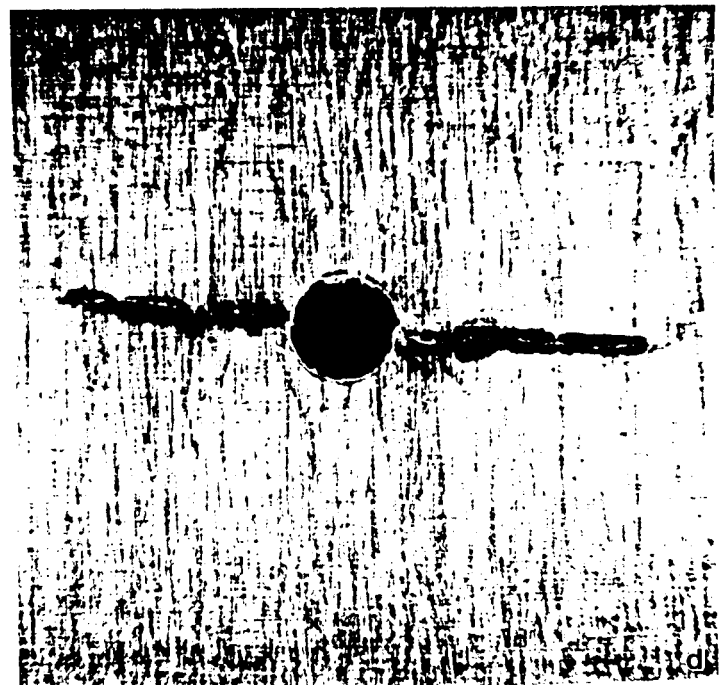
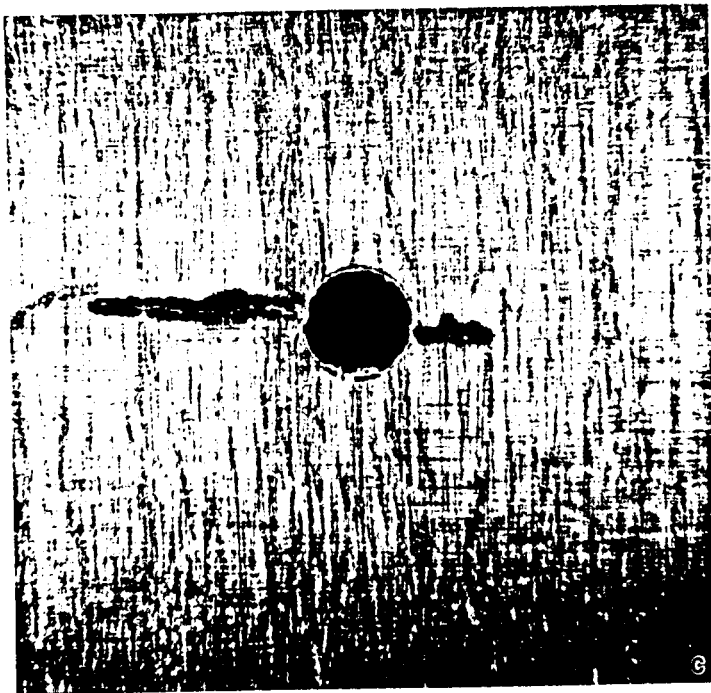
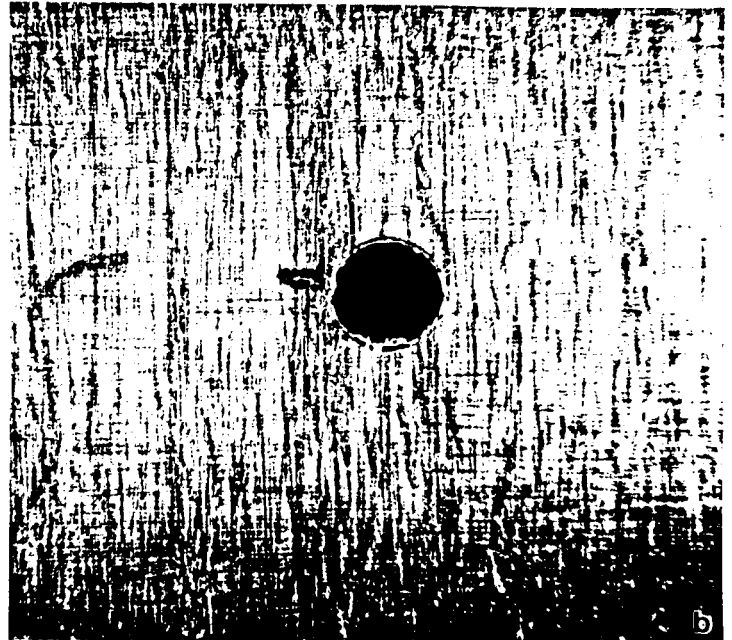
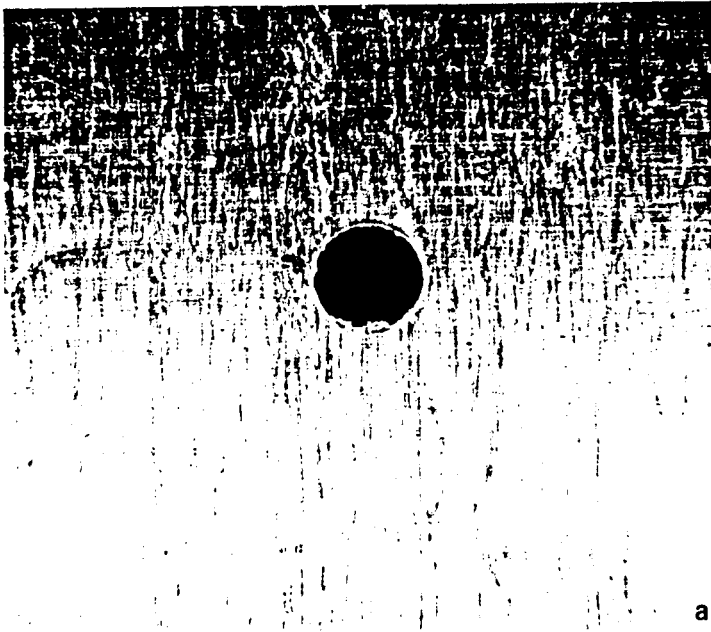


Fig. 4. Initiation and propagation of damage zone prior to compressive failure in an AS4/PEEK specimen. Hole diameter is 0.0625". Damage zone lengths are (a) 0.020", (b) 0.030", (c) 0.050" and 0.120", and (d) 0.140" and 0.140".

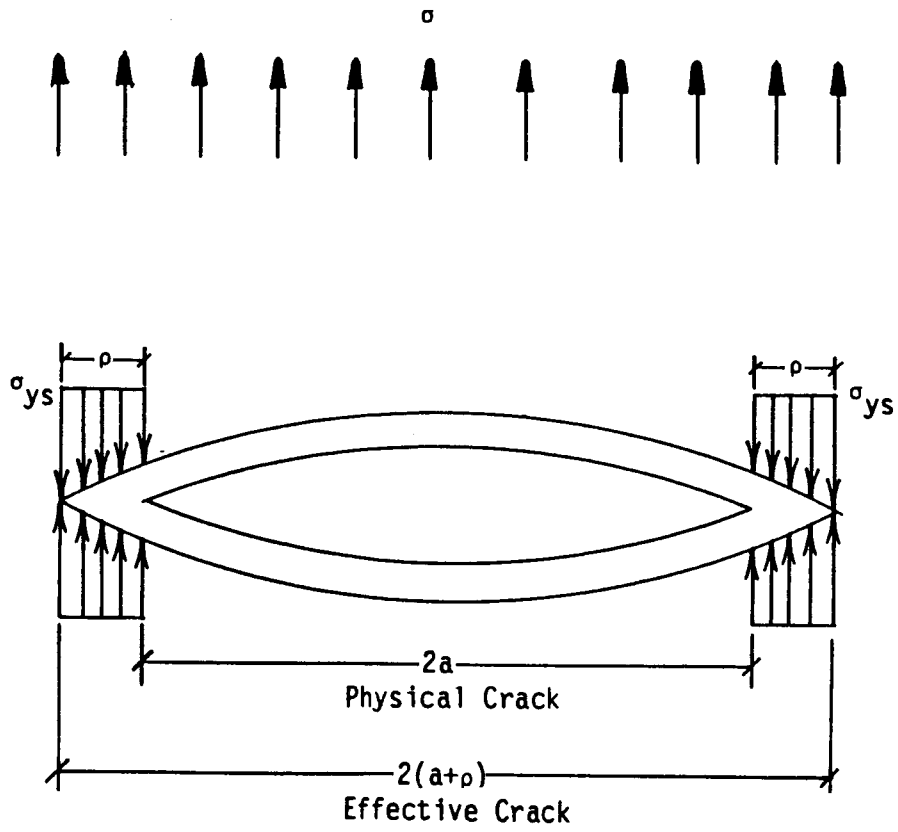


Fig. 5. Dugdale crack.

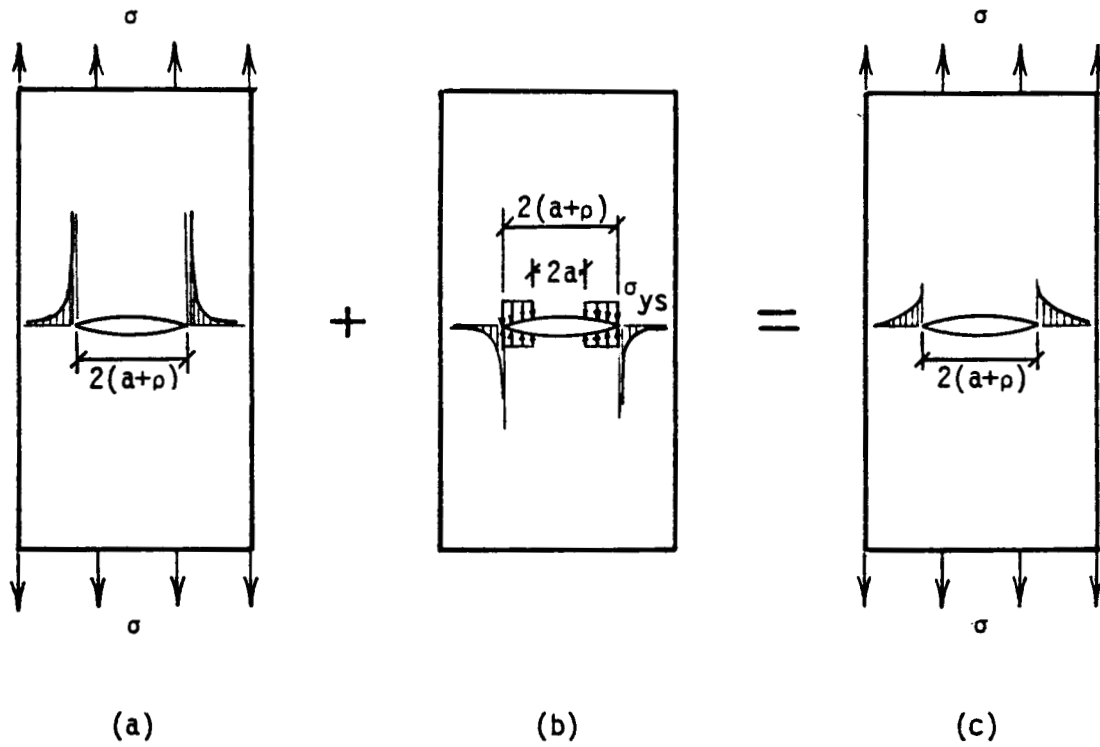


Fig. 6. Crack tip stress intensity. (a) Stress singularity at crack tip of tensile loaded coupon. (b) Compressive stress intensity at crack tip attributed to compressive surface stresses over the plastic zone. (c) Finite stress distribution in tensile loaded coupon.

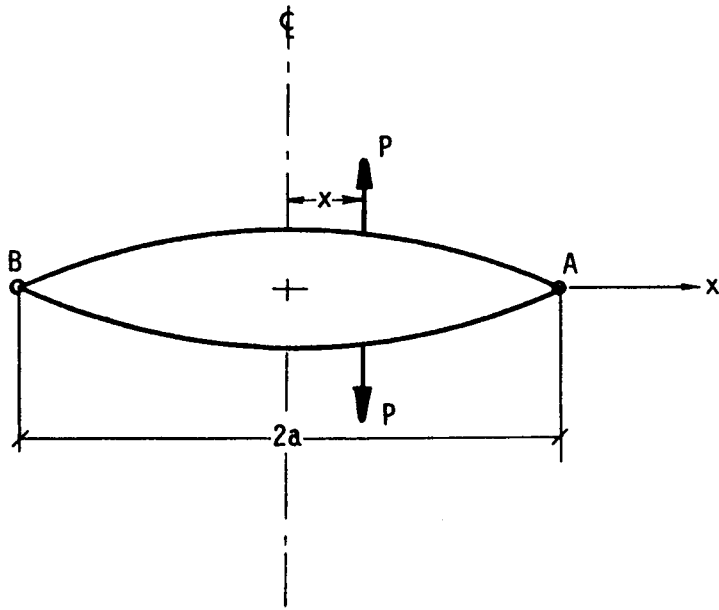


Fig. 7. Crack with applied wedge forces where P = force per unit plate thickness.

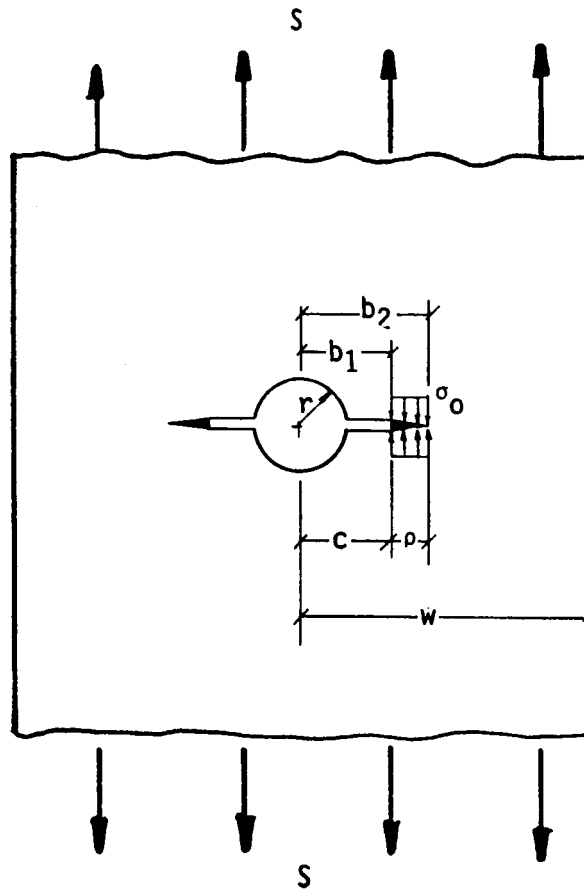


Fig. 8. Geometry for Newman's analysis.

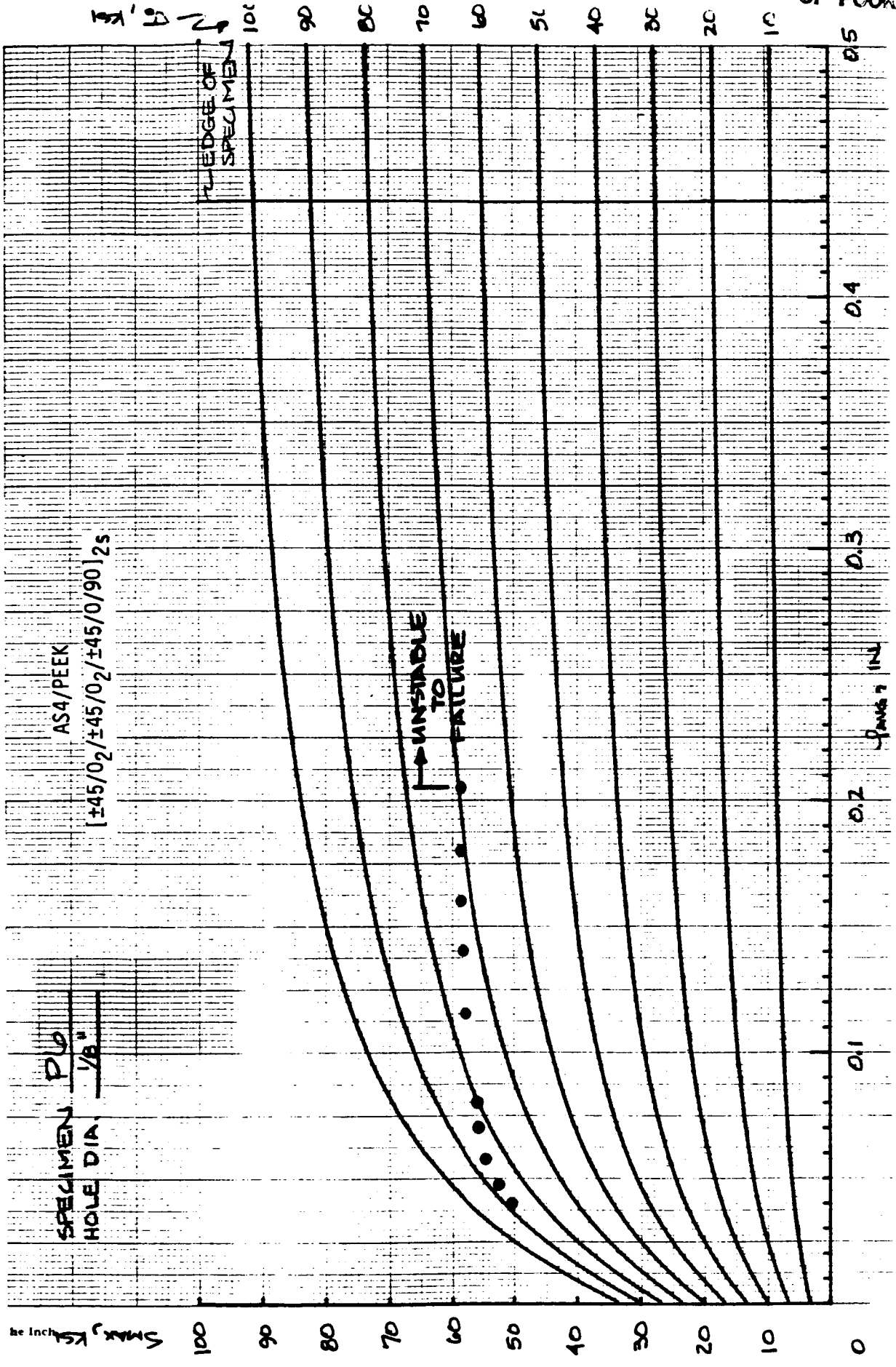
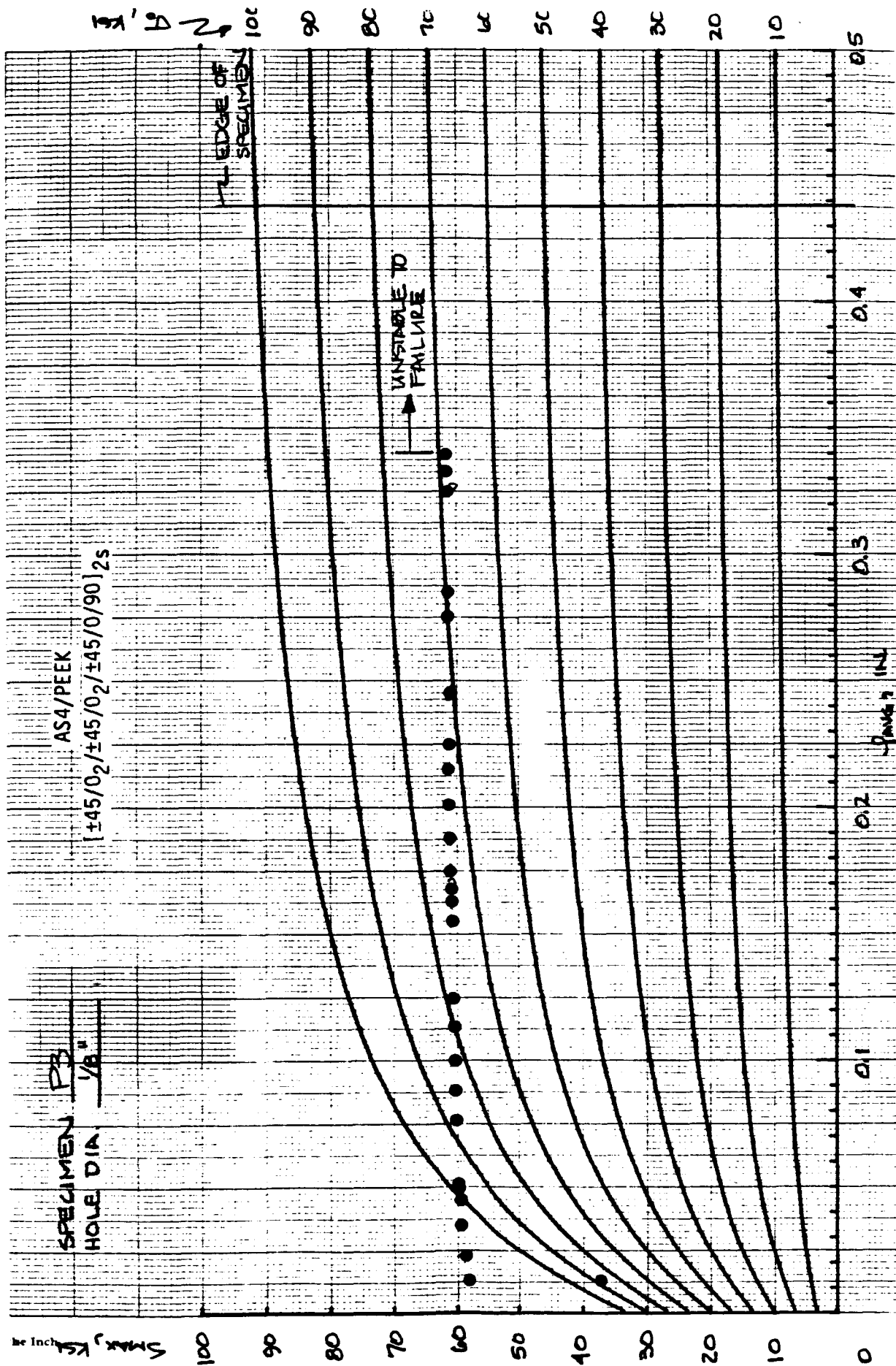


Fig. 9. Applied compressive stress vs. crush zone size for 0.125" hole.



ORIGINAL PAGE IS
OF POOR QUALITY

ORIGINAL PAGE IS
OF POOR QUALITY

Fig. 10. Applied compressive stress vs. crush zone size for 0.125" hole.

ORIGINAL PAGE IS
OF POOR QUALITY

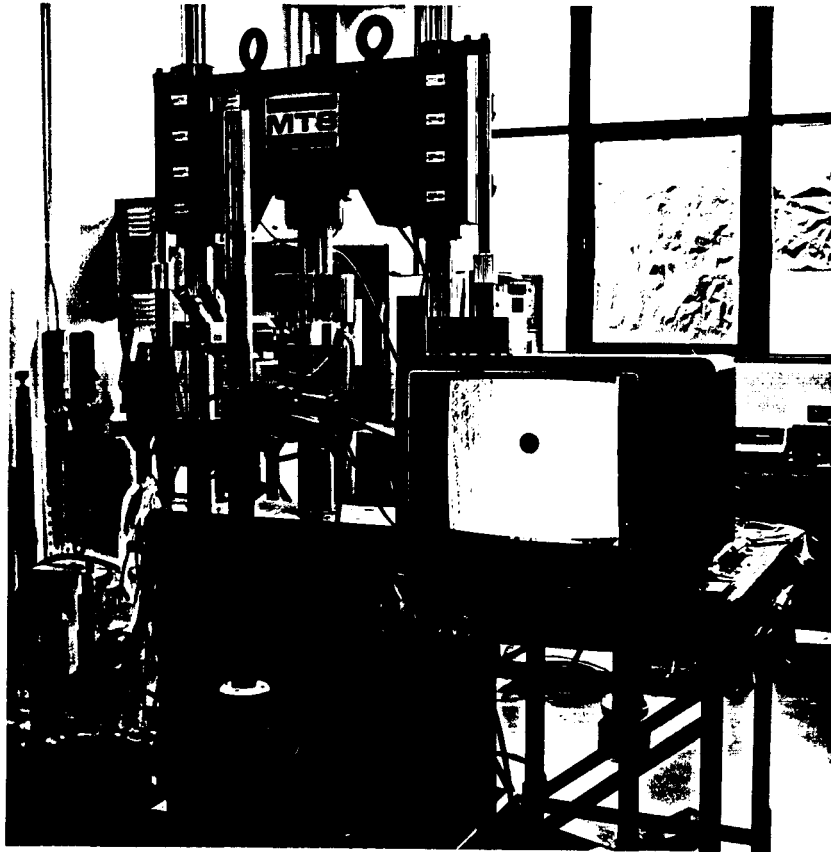


Fig. 11. Compression test facility with stereomicroscope and video attachments.

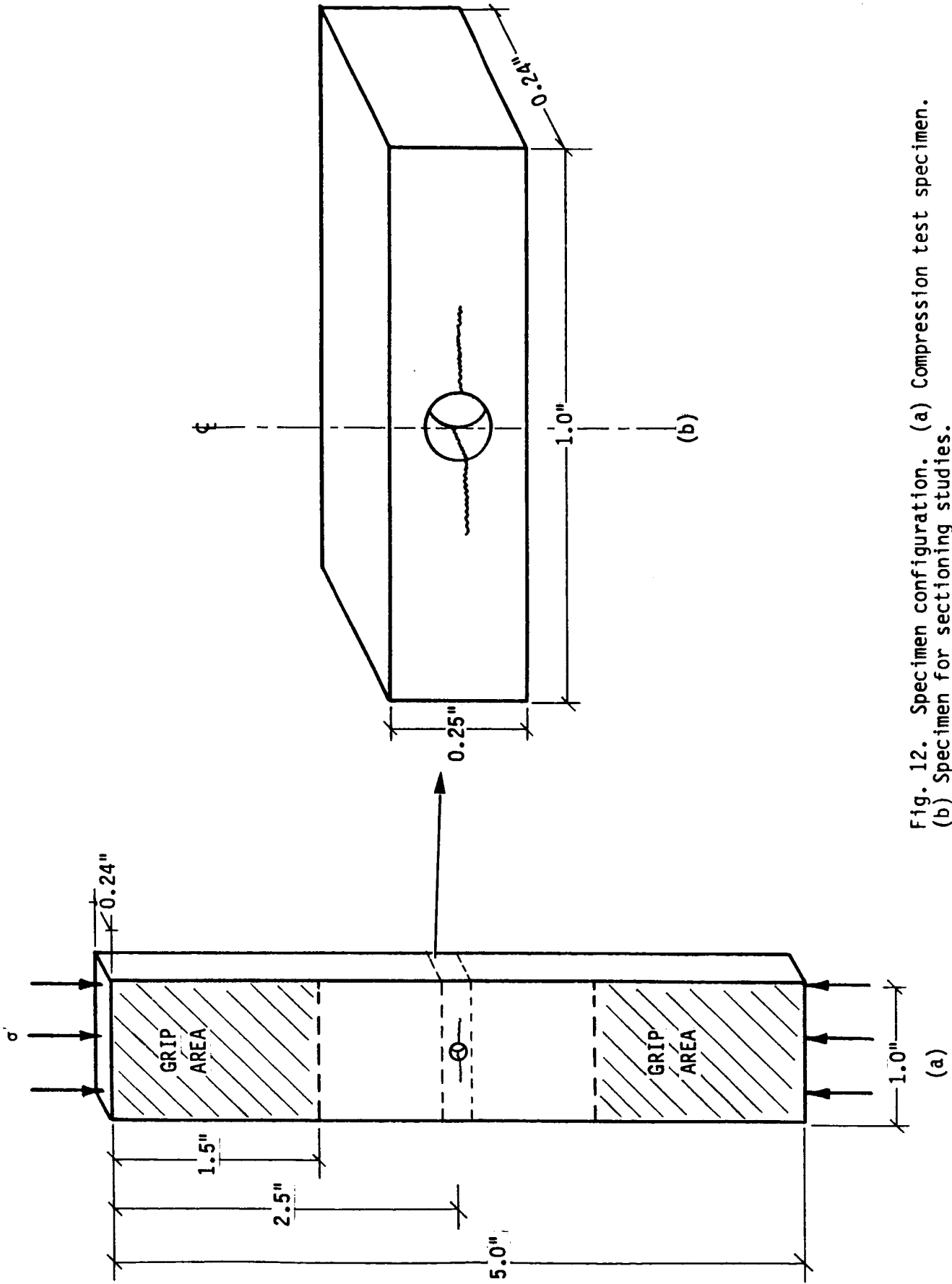


Fig. 12. Specimen configuration. (a) Compression test specimen. (b) Specimen for sectioning studies.